Study of additional jet activity in top quark pair production and decay at the LHC

Giuseppe Bevilacqua
Institute of Nuclear and Particle Physics, NCSR "Demokritos", 15341 Agia Paraskevi, Greece

Michele Lupattelli, Daniel Stremmer, and Małgorzata Worek
Institute for Theoretical Particle Physics and Cosmology, RWTH Aachen University, D-52056 Aachen, Germany

(Received 21 December 2022; accepted 12 May 2023; published 20 June 2023)

We report on the calculation of the next-to-leading order (NLO) QCD corrections to top quark pair production in association with two hard jets at the LHC. We take into account higher-order effects in both the production and decays of the top-quark pair. The latter are treated in the narrow width approximation and $t\bar{t}$ spin correlations are preserved throughout the calculation. This is the first time that such a complete study for this process is conducted at NLO in QCD. We present results for fiducial cross sections at the integrated and differential level. Furthermore, we investigate kinematic properties of the additional light jets and their distribution in the $pp \to t\bar{t}jj$ process. We examine jets in production and top-quark decays as well as the mixed contribution, where the two hardest non-b jets are present simultaneously in the production and decay processes.

DOI: 10.1103/PhysRevD.107.114027

I. INTRODUCTION

High precision theoretical predictions for $t\bar{t}$ production are crucial for precise measurements of the cross section and top-quark properties, which are carried out at the Large Hadron Collider (LHC) [1–4]. About half of the $t\bar{t}$ events, however, are accompanied by additional hard jet(s) arising from QCD radiation. Such events contribute to truly multiparticle final states, which are currently measured at the LHC [5–7]. Good understanding and excellent theoretical control of extra jet activity is a key for the entire top-quark physics program. In addition to its importance as a signal process, it turns out that the $t\bar{t}$ plus jets production can also be an important background process. For example, it is essential in Standard Model (SM) measurements of associated Higgs-boson production with a $t\bar{t}$ pair, where the Higgs boson decays into a $b\bar{b}$ pair. In addition, multiparticle final states originating from $t\bar{t}jj$ are abundantly predicted in various supersymmetric theories. Finally, anomalous production of additional jets accompanying a $t\bar{t}$ pair could be a sign of new physics. In all these scenarios, a small signal must be extracted from the overwhelming SM $t\bar{t}jj$ background.

For processes involving particles interacting via the strong interaction at least next-to-leading order (NLO) QCD predictions are needed to describe them in a reliable way. The NLO QCD corrections to $pp \to t\bar{t}jj$ production with stable top quarks have been calculated in Refs. [8,9]. In Ref. [10] $t\bar{t}$ pairs with up to two jets computed at NLO QCD have been consistently merged with a parton shower. In Ref. [11] theoretical predictions for the production of $t\bar{t}$ pairs with up to even three jets at NLO QCD were presented. Finally, in Ref. [12] the dominant NLO electroweak (EW) corrections have been incorporated into a parton shower framework for $t\bar{t}$ plus multijet production. In all of these studies, however, either only stable top quarks were considered or top-quark decays were treated in the parton shower approximation neglecting $t\bar{t}$ spin correlations either at LO or at NLO. The first case can provide information on the size of the higher-order effects in production rates but lacks a reliable description of fiducial-level cross sections. In the second case the parton shower, which incorporates the dominant soft-collinear logarithmic corrections, can approximate radiative effects in top-quark decays. The latter, however, are described by matrix elements formally accurate at LO only. Incorporating higher-order corrections in the decay processes already at the matrix element level would therefore be a further step towards a more complete description of the jet radiation pattern at NLO.

In this paper, we extend the previous studies for $pp \to t\bar{t}jj$ by adding higher order effects also to top-quark decays to match the level of accuracy already present in the production stage. Specifically, we calculate NLO QCD corrections to $t\bar{t}jj$ production and top-quark decays including $t\bar{t}$ spin correlations utilizing the narrow-width approximation

(NWA). This is the first time that such a complete study for this process is conducted at NLO QCD. The number of similar calculations for a $2 \to 6$ processes (the decay products of the Ws are not counted, because they do not couple to color charged states) at NLO in the NWA is rather limited. The $pp \to t\bar{t}b\bar{b}$ process is the only other case for which a full NLO description beyond the stable top-quark picture [13–16] is available [17]. Even NLO QCD predictions beyond the NWA have been calculated in Refs. [18,19]. For a less complicated $pp \to t\bar{t}j$ production the theoretical landscape is much more satisfactory as both the full off-shell and NWA descriptions are available [20–23]. Furthermore, NLO fixed-order $pp \to t\bar{t}b\bar{b}$ and $pp \to t\bar{t}j$ calculations have been also matched to parton shower programs [24–31], and top quark decays (in some cases spin correlated) have been included at LO accuracy. It would be beneficial to have a similar range of predictions for $pp \to t\bar{t}jj$ so that they all can ultimately be compared to understand their individual strengths and weaknesses. The first step in this direction is undertaken in this work.

II. PROCESS DEFINITION

In our studies we concentrate on the $pp \to t\bar{t}(jj) \to W^+W^-b\bar{b}jj \to \ell^+\ell^-\nu_\ell\bar{\nu}_\ell b\bar{b}jj$ decay chain, where $\ell^\pm = \mu^\pm, e^\pm$. We shall refer to the process as $t\bar{t}jj$, implicitly assuming that decays of the top quarks and W bosons are taken into account. By employing the dilepton decay channel we can distinguish the additional light jets from the hadronic top-quark decays. Having included jet emissions from various stages, we can explore their distribution and impact on the integrated and differential fiducial cross sections. To be as realistic as possible, we closely follow the event selection from the experimental analysis that has recently been carried out by the CMS collaboration [32].

In our calculation top quarks and $W^\pm$ gauge bosons are treated in the NWA. This approximation is obtained from the full cross section with unstable particles by taking the limit $\Gamma/m \to 0$. In this way all terms that are less singular than Γ^{-2} are consistently neglected, see e.g. Refs. [20,33–36]. Following closely the notation from Ref. [20] we write the formula for $\sigma^{\rm LO}_{t\bar{t}jj}$ in such a way that one can clearly show the different contributions:

$$d\sigma^{\rm LO}_{t\bar{t}jj} = \Gamma_t^{-2}\Big(\overbrace{d\sigma^{\rm LO}_{t\bar{t}jj}d\Gamma^{\rm LO}_{t\bar{t}}}^{\rm Production} + \overbrace{d\sigma^{\rm LO}_{t\bar{t}}d\Gamma^{\rm LO}_{t\bar{t}jj}}^{\rm Decay} + \overbrace{d\sigma^{\rm LO}_{t\bar{t}j}d\Gamma^{\rm LO}_{t\bar{t}j}}^{\rm Mix}\Big). \quad (1)$$

The first term in Eq. (1) describes $t\bar{t}jj$ production followed by top-quark decays. In this case light jets can occur only in the production stage. The middle term represents $t\bar{t}$ production followed by top-quark decays with two light jets appearing only in decays. The last term is responsible for the mixed contribution, where light jets appear simultaneously in the production and decay stage. We will refer to these contributions as *Production*, *Decay* and *Mix*, respectively.

A generalization to the $\sigma^{\rm NLO}_{t\bar{t}jj}$ case is given in Eq. (2), where α_s corrections to each term *Production*, *Decay* and *Mix* have been added. The symbol "virt" corresponds to virtual corrections and "real" denotes the case where one parton is allowed to be unresolved.

All theoretical predictions have been calculated with the HELAC-NLO Monte Carlo (MC) program [37]. Specifically, we compute the virtual corrections using HELAC-1LOOP [38–42], which has been extended to provide factorizable one-loop contributions for $pp \to t\bar{t} + X$ processes [43]. We cross-check our results with RECOLA [44–46], which is a computer program for the automated generation and numerical computation of tree and one-loop amplitudes. Because RECOLA is also able to provide one-loop matrix elements in the so-called double-pole approximation, see e.g. [47–49], it was straightforward to interface it to HELAC-NLO and use it in our case. Furthermore, we have implemented in RECOLA the random polarization method, which replaces the polarization state with a linear combination of helicity eigenstates [50–52]. This results in a drastic speed improvement, since now only one (random) polarization configuration must be calculated for each event. The singularities from soft or collinear parton emissions have been isolated via subtraction methods for NLO QCD calculations. We employ two independent subtraction schemes, the Catani-Seymour [53,54] and the Nagy-Soper scheme [52], which are both implemented in HELAC-DIPOLES [55]. In Refs. [17,43,56] the Catani-Seymour subtraction scheme has been extended to the NWA case to take into account gluon radiation in the decay of on-shell top quarks. In order to compute NLO QCD corrections to $pp \to t\bar{t}j(j)$ in the NWA, however, additional dipoles have been added since the additional processes $t \to bW^+gg$ and $t \to bW^+q\bar{q}$ are present. We have incorporated the final-initial dipoles for the splittings $g \to gg$ [20] and $g \to q\bar{q}$ with the top quark being the spectator. Additionally, the Nagy-Soper subtraction scheme has been adapted to deal with radiative corrections in the decay of on-shell top quarks. Until now, this subtraction scheme was not suitable for calculations in the NWA, thus, this is the first time we use it for this purpose. The Nagy-Soper subtraction has required several modifications, however, the technical description is beyond the scope of this paper.

$$\begin{aligned} d\sigma^{\rm NLO}_{t\bar{t}jj} = \Gamma_t^{-2}\Big(&\overbrace{(d\sigma^{\rm LO}_{t\bar{t}jj} + d\sigma^{\rm virt}_{t\bar{t}jj} + d\sigma^{\rm real}_{t\bar{t}jjj})d\Gamma^{\rm LO}_{t\bar{t}}}^{\rm Production} + \overbrace{d\sigma^{\rm LO}_{t\bar{t}}(d\Gamma^{\rm LO}_{t\bar{t}jj} + d\Gamma^{\rm virt}_{t\bar{t}jj} + d\Gamma^{\rm real}_{t\bar{t}jjj})}^{\rm Decay} \\ &+ \underbrace{d\sigma^{\rm LO}_{t\bar{t}j}d\Gamma^{\rm LO}_{t\bar{t}j} + d\sigma^{\rm LO}_{t\bar{t}jj}d\Gamma^{\rm virt}_{t\bar{t}} + d\sigma^{\rm virt}_{t\bar{t}}d\Gamma^{\rm LO}_{t\bar{t}jj} + d\sigma^{\rm virt}_{t\bar{t}j}d\Gamma^{\rm LO}_{t\bar{t}j} + d\sigma^{\rm LO}_{t\bar{t}j}d\Gamma^{\rm virt}_{t\bar{t}j} + d\sigma^{\rm real}_{t\bar{t}jj}d\Gamma^{\rm real}_{t\bar{t}j} + d\sigma^{\rm real}_{t\bar{t}j}d\Gamma^{\rm real}_{t\bar{t}jj}}_{\rm Mix}\Big). \end{aligned} \quad (2)$$

The set of subtraction terms needed in both schemes for calculations in the NWA is now completed and HELACDIPOLES can perform NLO QCD calculations for $pp \to t\bar{t}$ processes with an arbitrary number of colorless/colorful final states.

III. LHC SETUP

We present results for the LHC with $\sqrt{s} = 13$ TeV. The SM parameters are given within the G_μ scheme with $G_\mu = 1.1663787 \times 10^{-5}\,\text{GeV}^{-2}$, $m_Z = 91.1876\,\text{GeV}$, $m_W = 80.379$ GeV and $\Gamma_W^{\text{NLO}} = 2.0972$ GeV. The top quark mass is set to $m_t = 172.5$ GeV. All other particles, including bottom quarks and leptons, are considered massless. For the LO and NLO top-quark width, based on Refs. [57,58], we use the following values:

$$\begin{aligned} \Gamma_t^{\text{LO}} &= 1.4806842 \text{ GeV}, \\ \Gamma_t^{\text{NLO}} &= 1.3535983 \text{ GeV}. \end{aligned} \tag{3}$$

We treat Γ_t as a fixed parameter and its NLO value corresponds to $\mu_R = m_t$.[1] We work in the five-flavor scheme but neglect bottom quarks in the initial state. We use an exclusive setup by requiring exactly two b jets in the final state, where we define a b jet as a jet with nonzero net bottomness. For example, a jet containing a single b quark (or b antiquark) plus a gluon is considered to be a b jet. On the contrary, a jet containing $b\bar{b}$ is labeled as a light jet, see e.g. Refs. [19,36]. Therefore, in the real emission part of the calculation we do not encounter subprocesses with one bottom quark in the initial state like for example $bg \to t\bar{t}bgg$ or $bg \to t\bar{t}bq\bar{q}$, where $q = u, d, c, s$ that would lead to the underlining $bg \to t\bar{t}bg$ configuration at the Born level. On the other hand, $gg/q\bar{q} \to t\bar{t}b\bar{b}g$ subprocesses, with $gg/q\bar{q} \to t\bar{t}gg$ underlining Born contributions, are consistently included in our calculations. The remaining b-initiated subprocesses, $b\bar{b}/\bar{b}b \to t\bar{t}gg$ and $b\bar{b}/\bar{b}b \to t\bar{t}q\bar{q}$, are about 0.01% of the total LO cross section and thus numerically negligible. In order to check the correctness of our calculations, as mentioned earlier, two independent subtraction schemes have been employed. We found agreement on a per mille level between the results obtained with the two schemes. The LHAPDF interface [59] is used to provide an access to parton distribution functions (PDFs) and we employ the NLO NNPDF3.1 PDF set [60] at LO and NLO. The running of the strong coupling constant is performed in both cases with two-loop accuracy. We provide additionally the results for MSHT20 [61] and CT18 [62]. The three PDF sets, which we employ, are recommended for SM calculations by the PDF4LHC Working Group [63]. To cluster final state partons into jets we use the $anti-k_T$ jet algorithm [64] with $R = 0.4$. We require exactly two opposite-sign charged leptons, two b jets and at least two light jets. Leptons are required to have $p_{T\ell} > 20$ GeV, $|y_\ell| < 2.4$, $\Delta R_{\ell\ell} > 0.4$ and $M_{\ell\ell} > 20$ GeV, where $\ell^\pm = e^\pm, \mu^\pm$ as mentioned before. Flavored jets with $p_{Tb} > 30$ GeV and $|y_b| < 2.4$ are selected and only b jets that are well separated from leptons, $\Delta R_{b\ell} > 0.4$, are taken into account. Light jets are required to have $p_{Tj} > 40$ GeV and $|y_j| < 2.4$. They have to be isolated from leptons and b jets according to $\Delta R_{j\ell} > 0.4$ and $\Delta R_{jb} > 0.8$. The latter cut minimizes gluon radiation from top-quark decays. The default renormalization (μ_R) and factorization (μ_F) scale settings are

$$\mu_R = \mu_F = \mu_0 = \frac{H_T}{2}, \tag{4}$$

where H_T is calculated according to

$$H_T = \sum_{i=1}^{2} p_{T\ell_i} + \sum_{i=1}^{2} p_{Tj_i} + \sum_{i=1}^{2} p_{Tb_i} + p_T^{\text{miss}}, \tag{5}$$

and p_T^{miss} is the missing transverse momentum constructed of two neutrinos which are present in the $pp \to t\bar{t}jj$ process ($\nu_\ell, \bar{\nu}_\ell$). In all cases, we estimate scale uncertainties by performing a seven-point scale variation around the central value of the scale (μ_0). Specifically, we vary μ_R and μ_F independently in the following range:

$$\begin{aligned} (\mu_R, \mu_F) = [&(2\mu_0, 2\mu_0), (2\mu_0, \mu_0), (\mu_0, 2\mu_0), (\mu_0, \mu_0), \\ &(\mu_0/2, \mu_0), (\mu_0, \mu_0/2), (\mu_0/2, \mu_0/2)], \end{aligned} \tag{6}$$

and choose the minimum and maximum of the resulting cross sections.

IV. RESULTS

The integrated LO and NLO fiducial cross sections for $pp \to t\bar{t}jj$ are shown in Table I. The LO cross section is dominated by the gg channel with the $\sigma_{gg}^{\text{LO}} = 561.1(2)$ fb (65%) contribution. It is followed by the gq channel with $\sigma_{gq}^{\text{LO}} = 272.6(1)$ fb (31%), where gq stands for gq,

TABLE I. Integrated fiducial cross section at LO and NLO for the $pp \to t\bar{t}jj$ process at the LHC with $\sqrt{s} = 13$ TeV. Results are given for the default cuts with $\Delta R_{jb} > 0.8$. The full result as well as *Production*, *Decay* and *Mix* contributions are shown. Theoretical uncertainties from scale variations and MC integration errors (in parentheses) are also displayed.

i	σ^{LO} [fb]	σ^{NLO} [fb]	$\sigma_i^{\text{LO}}/\sigma_{\text{Full}}^{\text{LO}}$	$\sigma_i^{\text{NLO}}/\sigma_{\text{Full}}^{\text{NLO}}$
Full	$868.8(2)^{+60\%}_{-35\%}$	$1225(1)^{+1\%}_{-14\%}$	1.00	1.00
Production	$843.2(2)^{+60\%}_{-35\%}$	$1462(1)^{+12\%}_{-19\%}$	0.97	1.19
Mix	25.465(5)	−236(1)	0.029	−0.19
Decay	0.2099(1)	0.1840(8)	0.0002	0.0002

[1]While calculating the scale dependence for the NLO cross section we keep Γ_t^{NLO} fixed. The error introduced by this treatment is however small, and particularly for two scales $\mu_R = 2m_t$ and $\mu_R = m_t/2$ is at the level of 1% only.

TABLE II. Integrated fiducial cross section at LO and NLO for the $pp \to t\bar{t}jj$ process at the LHC with $\sqrt{s} = 13$ TeV. Results are given for the default cuts but with $\Delta R_{jb} > 0.4$. The full result as well as *Production*, *Decay* and *Mix* contributions are shown. Theoretical uncertainties from scale variations and MC integration errors (in parentheses) are also displayed.

i	$\sigma^{\rm LO}$ [fb]	$\sigma^{\rm NLO}$ [fb]	$\sigma_i^{\rm LO}/\sigma_{\rm Full}^{\rm LO}$	$\sigma_i^{\rm NLO}/\sigma_{\rm Full}^{\rm NLO}$
Full	$1074.5(3)^{+60\%}_{-35\%}$	$1460(1)^{+1\%}_{-13\%}$	1.00	1.00
Production	$983.1(3)^{+60\%}_{-35\%}$	$1662(1)^{+11\%}_{-18\%}$	0.91	1.14
Mix	89.42(3)	−205(1)	0.083	−0.14
Decay	1.909(1)	2.436(6)	0.002	0.002

qg, $g\bar{q}$ and $\bar{q}g$. The smallest contribution comes from the $q\bar{q}$ channel with $\sigma^{\rm LO}_{q\bar{q}} = 35.10(1)$ fb (4%), where $q\bar{q} \in (q\bar{q}, \bar{q}q, qq, \bar{q}\,\bar{q}, qq', \bar{q}\bar{q}', q\bar{q}', \bar{q}q')$. The $\mathcal{K}$ factor for the full NWA calculation, defined as $\mathcal{K} = \sigma^{\rm NLO}_{\rm Full}/\sigma^{\rm LO}_{\rm Full}$, is $\mathcal{K} = 1.41$. Thus, $\mathcal{O}(\alpha_s)$ corrections are of medium size. When NLO QCD corrections are included, a reduction in the dependence on the unphysical μ_R and μ_F scales from 60% down to 14%, thus of more than a factor of 4, is observed. In order to examine how light jets are distributed we additionally provide in Table I *Production*, *Decay* and *Mix* contributions defined according to Eqs. (1) and (2). At LO the dominant input comes from *Production* (97%) and it is followed by *Mix* (3%), whereas the *Decay* part is negligible. The *Mix* contribution increases from 3% to 8% when the ΔR_{jb} cut is set to 0.4 instead of 0.8 (see Table II). Nevertheless, this contribution might be safely disregarded given that scale uncertainties at this perturbative order are much larger. Once NLO QCD corrections are included not only the relative size of *Mix* increases up to 19%, but also its sign is reversed. This behavior is driven by radiative corrections to the decays of $t\bar{t}jj$, denoted by $d\sigma^{\rm LO}_{t\bar{t}jj} d\Gamma^{\rm virt}_{t\bar{t}}$ and $d\sigma^{\rm real}_{t\bar{t}jj} d\Gamma^{\rm real}_{t\bar{t}j}$ in Eq. (2), which are known to be negative and increase (in absolute values) when the ΔR_{jb} cut is reduced to 0.4. However, other components of the *Mix* part, notable $d\sigma^{\rm LO}_{t\bar{t}j} d\Gamma^{\rm LO}_{t\bar{t}j}$ and its direct NLO QCD corrections are positive and more sensitive to this cut. Consequently, the overall size of *Mix* reduces to 14% for $\Delta R_{jb} > 0.4$ (see Table II).

From the considerations above, we can conclude that neither the size nor the sign of the *Mix* contribution can be reliably estimated on the basis of LO predictions. In addition, its sensitivity to higher-order effects is very dependent on the fiducial phase-space cuts. Finally, omitting the *Mix* part can lead to rather misleading conclusions about the size of higher-order corrections and theoretical uncertainties. Thus, unless full NLO QCD corrections are carefully incorporated into the NWA computations of $pp \to t\bar{t}jj$, it is not clear to what extent various predictions available in literature can be trusted. If only the *Production* contribution to $t\bar{t}jj$ is taken into account, under question could be not only the modeling of top-quark decays but also the extrapolation of the $t\bar{t}jj$ fiducial predictions to the full phase space.

To investigate this further, we have compared our NLO QCD result in the full NWA ($\sigma^{\rm NLO}_{\rm Full}$) to the prediction that includes NLO QCD corrections to $t\bar{t}jj$ production only (i.e. with two light jets present in the production stage) while top-quark decays are modeled with LO accuracy. We refer to this result as $\sigma^{\rm NLO}_{\rm Production\,LO_{Decay}}$. For the larger value of the ΔR_{jb} cut the two results are almost identical, whereas for $\Delta R_{jb} > 0.4$ a difference of only 5% is observed. We therefore conclude that when comparing to $\sigma^{\rm NLO}_{\rm Production\,LO_{Decay}}$ the inclusion of the *Mix* contribution at NLO leads to rather small differences in the central value for our setup. However, we gain in theoretical accuracy, reducing scale uncertainties by about 5%.

In Fig. 1 we show the size of *Production*, *Decay* and *Mix* relative to $\sigma^{\rm NLO}_{\rm Full}$ as a function of H_T^{had}, defined as

$$H_T^{had} = \sum_{i=1}^{2} p_{Tj_i} + \sum_{i=1}^{2} p_{Tb_i}, \tag{7}$$

and $\Delta R_{j_1 j_2}$. Also at the differential level the *Decay* contribution is negligible. However, the negative *Mix* contribution has nontrivial dependence on kinematics. For H_T^{had} its importance increases (in absolute values) at the beginning of the spectrum and from around 400 GeV it stabilizes at around 25%. For $\Delta R_{j_1 j_2}$ the *Mix* part is particularly important for the $\Delta R_{j_1 j_2} \leq 1$ phase-space region, which represents the bulk of the distribution (see also Fig. 3), especially when the default cut $\Delta R_{jb} > 0.8$ is employed. Indeed, for small values of $\Delta R_{j_1 j_2}$ the *Mix* contribution amounts to −23%, whereas for $\Delta R_{j_1 j_2} \approx 3$ we obtained −17%. Beyond that, the difference between the two cases, $\Delta R_{jb} > 0.8$ (solid line) and $\Delta R_{jb} > 0.4$ (dashed line), is clearly visible for the small p_T region of H_T^{had} and for the back-to-back configurations in the case of $\Delta R_{j_1 j_2}$. In the latter case, even though the *Mix* contribution is still negative, it is reduced to 8% in the case of $\Delta R_{jb} > 0.4$.

Also at the differential cross-section level, a comparison between $\sigma^{\rm NLO}_{\rm Full}$ and $\sigma^{\rm NLO}_{\rm Production\,LO_{Decay}}$ has been carried out. In this case, differences of up to 15%–20% are observed for various observables that we have examined. Both dimensionless and dimensionful observables as well as various phase-space regions are affected. As an example, we show in Fig. 2 the transverse momentum of the $j_1 j_2$ system ($p_{T,j_1 j_2}$) as well as the azimuthal angle difference between these two light jets ($\Delta\phi_{j_1 j_2}$) at NLO in QCD for the default cuts but with $\Delta R_{jb} > 0.4$. In the upper panels we show the absolute NLO predictions for the full NWA and for the NWA case with LO top-quark decays and two light jets in the production stage only. In the lower panels the differential $\sigma^{\rm NLO}_{\rm Full}/\sigma^{\rm NLO}_{\rm Production\,LO_{Decay}}$ ratio is displayed together with the corresponding uncertainty bands. The error band is built bin by bin by employing, similarly to the integrated fiducial cross-section case, a seven-point scale variation. In addition to the shape differences already mentioned, we can observe

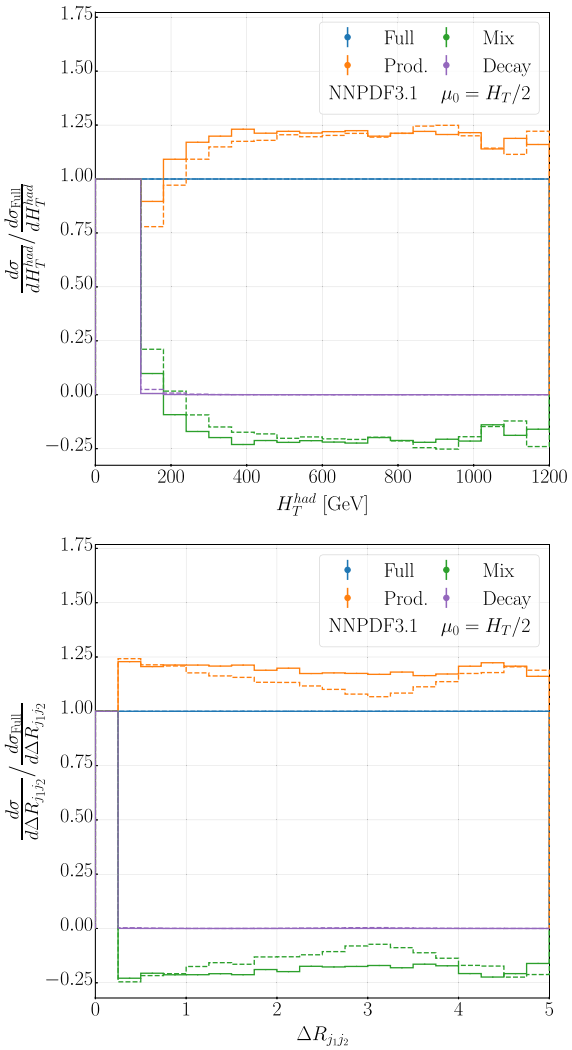

FIG. 1. Fraction of events when the two light jets come from $t\bar{t}$ production or $t \to Wb$ decays as a function of H_T^{had} and $\Delta R_{j_1 j_2}$. Also shown is the mixed contribution where they are emitted simultaneously in the production and top-quark decays. NLO QCD results are shown for the $pp \to t\bar{t}jj$ process at the LHC with $\sqrt{s} = 13$ TeV. They are given for the default cuts with $\Delta R_{jb} > 0.8$ (solid line) and $\Delta R_{jb} > 0.4$ (dashed line).

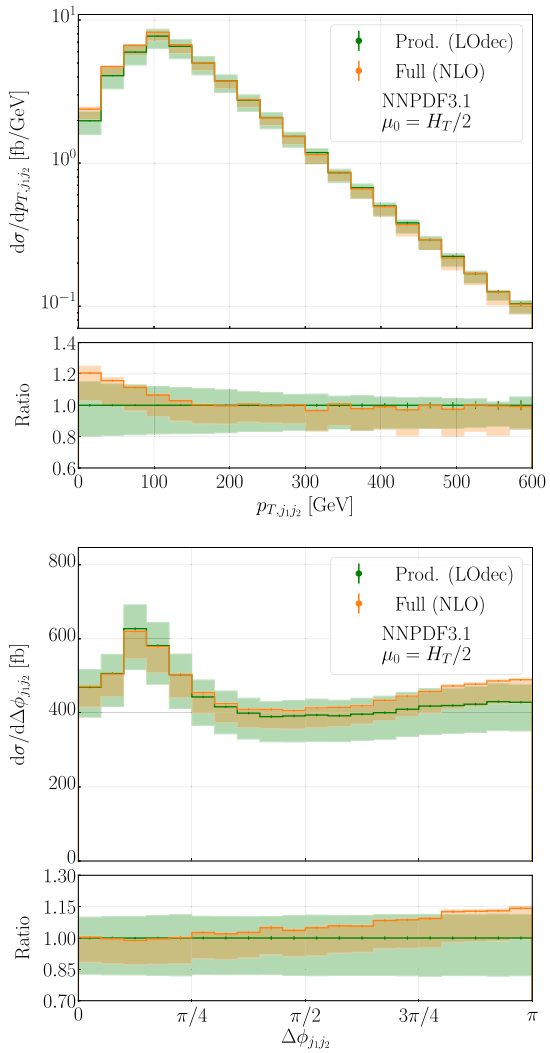

FIG. 2. Differential cross-section distribution at NLO in QCD as a function of $p_{T,j_1 j_2}$ and $\Delta\phi_{j_1 j_2}$ for the $pp \to t\bar{t}jj$ process at the LHC with $\sqrt{s} = 13$ TeV. Results are given for the default cuts but with $\Delta R_{jb} > 0.4$. Two different theoretical descriptions are employed. The orange curve corresponds to the full NWA result and the green curve to the NWA prediction with LO top-quark decays and two light jets in the production stage only. The corresponding uncertainty bands are also shown. The lower panels display the differential $\sigma^{NLO}_{Full} / \sigma^{NLO}_{Production\,LO_{Decay}}$ ratio with the corresponding uncertainty bands.

reduced theoretical uncertainties for the full NWA result. We can thus clearly see the importance of including the full NLO QCD corrections in the NWA calculations for the $pp \to t\bar{t}jj$ process.

The second source of theoretical systematic uncertainties comprises PDF uncertainties. For $pp \to t\bar{t}jj$ they are of the order of 1.3% for our default NNPDF3.1 PDF set. Furthermore, for the MSHT20 PDF set we obtain $\sigma^{NLO}_{MSHT20} = 1212(1)$ fb, whereas for CT18 we have $\sigma^{NLO}_{CT18} = 1197(1)$ fb. The corresponding internal PDF uncertainties are 2.1% and 2.9%. By comparing $\sigma^{NLO}_{NNPDF3.1}$ with σ^{NLO}_{MSHT20} and σ^{NLO}_{CT18}, relative differences in the range of 1.1%–2.3% are observed, which are consistent with the size of the internal PDF uncertainties. In general, PDF uncertainties are well below theoretical uncertainties from scale variations.

While the size of the NLO QCD corrections to the integrated fiducial cross section is certainly of interest, it is crucial to examine the higher-order effects to various differential cross-section distributions. In Fig. 3 we display four examples: H_T^{had}, $\Delta R_{j_1 j_2}$, y_{b_1} (the hardest b-jet's rapidity) and $\Delta R_{b_1 b_2}$. Results are given for the default cuts with $\Delta R_{jb} > 0.8$. For each plot the upper panels show absolute LO and NLO predictions together with the corresponding scale uncertainty bands. The lower panels display the differential $\mathcal{K}$ factor. The LO and NLO uncertainty bands normalized to the LO central value are

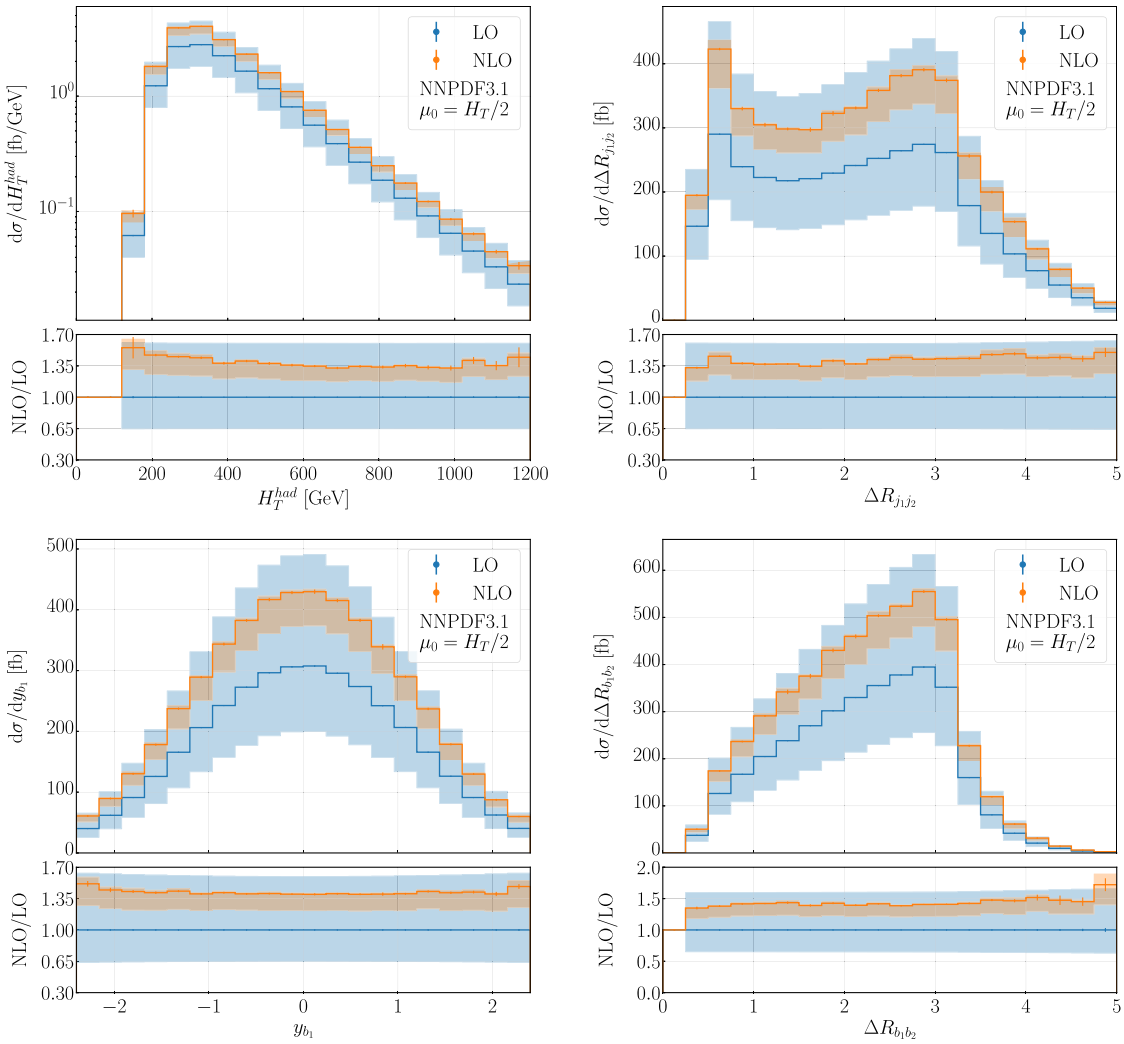

FIG. 3. Differential cross-section distributions at NLO in QCD as a function of H_T^{had}, $\Delta R_{j_1j_2}$, y_{b_1} and $\Delta R_{b_1b_2}$ for the $pp \to t\bar{t}jj$ process at the LHC with $\sqrt{s} = 13$ TeV. Results are given for the default cuts with $\Delta R_{jb} > 0.8$. The blue curve corresponds to the LO and the red curve to the NLO result. The corresponding uncertainty bands are also shown. The lower panels display the differential $\mathcal{K}$ factor together with uncertainty bands.

also displayed. Similar to the integrated fiducial cross sections we find a significantly reduced dependence on the choice of μ_F and μ_R also at the differential level. Specifically, for all observables we obtain LO theoretical uncertainties of the order of 60% while at NLO they are maximally up to 15%, giving a reduction by a factor of 4. Moreover, scale dependence bands for LO and NLO predictions overlap nicely, indicating a well behaved perturbative convergence. It should be noted here that we observe rather asymmetric theoretical uncertainties analogous to the case of the integrated fiducial cross section. In such a situation, the maximum of the two values in each bin should be taken as the final theoretical error estimate. An alternative would be to symmetrize the two values, but this approach might underestimate the final error, which will only be known once NNLO QCD corrections to the $pp \to t\bar{t}jj$ process, with all three contributions *Production*, *Decay* and *Mix* included, are available. We would like to emphasize here that the scale variation is by no means a rigorous way to assess the true theoretical uncertainty. At best, it might only give an indication of the full uncertainty which is due to the not yet calculated higher order corrections. As for the NLO QCD corrections to the differential cross-section distributions, they are significant as they are in the range of 30%–50%. An appropriate global $\mathcal{K}$ factor cannot therefore be applied to all LO predictions to well approximate NLO predictions. Consequently, the complete NLO QCD corrections should be consistently incorporated to all differential cross-section distributions.

To show the potential of HELAC-NLO we present results for $pp \to t\bar{t} + nj$ in the dilepton channel, with $n = 0, 1, 2$, in the form of fiducial cross section ratios, defined as $\mathcal{R}_n = \sigma_{t\bar{t}+nj}/\sigma_{t\bar{t}+(n-1)j}$. They are displayed in Table III for

TABLE III. LO and NLO cross section ratios for the $pp \to t\bar{t}jj$ process at the LHC with $\sqrt{s} = 13$ TeV. Results are given for the default cuts with $\Delta R_{jb} > 0.8$. In the last column the expanded NLO cross section ratio to first order in α_s is also given. Theoretical uncertainties from scale variations, which are taken as correlated, are also displayed. MC integration errors are at the per mill level.

$\mathcal{R}_n$	$\mathcal{R}^{\mathrm{LO}}$	$\mathcal{R}^{\mathrm{NLO}}$	$\mathcal{R}^{\mathrm{NLO}}_{\mathrm{exp}}$
$\mathcal{R}_1 = \sigma_{t\bar{t}j}/\sigma_{t\bar{t}}$	$0.3686^{+12\%}_{-10\%}$	$0.3546^{+0\%}_{-5\%}$	$0.3522^{+0\%}_{-3\%}$
$\mathcal{R}_2 = \sigma_{t\bar{t}jj}/\sigma_{t\bar{t}j}$	$0.2539^{+11\%}_{-9\%}$	$0.2660^{+0\%}_{-5\%}$	$0.2675^{+0\%}_{-2\%}$

our default setup up to a modification in the definition of $\mu_0 = H_T/2$ for $pp \to t\bar{t}(j)$. Theoretical uncertainties from scale variations are taken as correlated. The internal PDF uncertainties are evaluated in a similar fashion as for the integrated fiducial cross section that allow us to properly account for cross-correlations between the two processes considered for the numerator and the denominator of $\mathcal{R}_{1,2}$. Nevertheless, they are only up to 0.5%. The last column, $\mathcal{R}^{\mathrm{NLO}}_{\mathrm{exp}}$, shows a consistent expansion of $\mathcal{R}$ in α_s. In both cases, the difference between $\mathcal{R}^{\mathrm{NLO}}_{\mathrm{exp}}$ and $\mathcal{R}^{\mathrm{NLO}}$ is similar in size as the MC errors. Thus, $\mathcal{R}_{1,2}$ are very stable and precise observables that should be measured at the LHC. Indeed, a judicious choice of μ_R, μ_F allows us to obtain 2%–3% precision for $\mathcal{R}^{\mathrm{NLO}}_{1,2}$. Until now, such precise predictions were reserved only for $pp \to t\bar{t}$ at NNLO QCD.

V. CONCLUSIONS

We have computed, for the first time, the complete set of NLO QCD corrections to $pp \to t\bar{t}jj$ including top-quark decays at the LHC in the NWA. Our calculation shows that NLO QCD corrections to $pp \to t\bar{t}jj$ with realistic final states play an important role as they substantially increase the SM prediction and significantly decrease the dominant scale uncertainty. An important finding of this paper is the magnitude and the sign of the *Mix* contribution. The latter is normally omitted in various studies for $pp \to t\bar{t}jj$. As important as it is, if not properly accounted for, it can affect the modeling of top-quark decays and the extrapolation to full phase space with existing MC event generators. This is especially true when considering various differential cross-section distributions where differences between $\sigma^{\mathrm{NLO}}_{\mathrm{Full}}$ and $\sigma^{\mathrm{NLO}}_{\mathrm{Production\,LO_{Decay}}}$ up to 15%–20% are observed.

We conclude by saying that it would be beneficial to make a comparison between the results obtained in this work and those reported in literature. Such a comparison could assess the extent to which parton shower effects can reproduce all the contributions required at the NLO level in QCD for the $pp \to t\bar{t}jj$ process. In addition, it could help to identify regions of phase space for specific observables that are indeed sensitive to resummed dominant soft-collinear logarithmic corrections from parton showers, which are absent in our fixed-order predictions for this process. We plan to carry out such comparisons in the future.

ACKNOWLEDGMENTS

The work of M. L., D. S. and M. W. was supported by the Deutsche Forschungsgemeinschaft (DFG) under Grant No. 396021762–TRR 257: *P3H—Particle Physics Phenomenology after the Higgs Discovery* and by the DFG under Grant No. 400140256–GRK 2497: *The physics of the heaviest particles at the Large Hadron Collider*. Support by a grant of the Bundesministerium für Bildung und Forschung (BMBF) is additionally acknowledged. G. B. was supported by the Hellenic Foundation for Research and Innovation (HFRI) under the "2nd Call for H.F.R.I. Research Projects to support Faculty Members & Researchers" (Project No. 02674 HOCTools-II). Simulations were performed with computing resources granted by RWTH Aachen University under Projects No. p0020216, No. rwth0414 and No. rwth0846.

[1] A. M. Sirunyan *et al.* (CMS Collaboration), J. High Energy Phys. 02 (2019) 149.
[2] A. M. Sirunyan *et al.* (CMS Collaboration), Eur. Phys. J. C **80**, 658 (2020).
[3] A. M. Sirunyan *et al.* (CMS Collaboration), Phys. Rev. D **100**, 072002 (2019).
[4] G. Aad *et al.* (ATLAS Collaboration), Eur. Phys. J. C **80**, 528 (2020).
[5] M. Aaboud *et al.* (ATLAS Collaboration), Eur. Phys. J. C **77**, 220 (2017).
[6] M. Aaboud *et al.* (ATLAS Collaboration), J. High Energy Phys. 10 (2018) 159.
[7] A. M. Sirunyan *et al.* (CMS Collaboration), J. High Energy Phys. 07 (2020) 125.
[8] G. Bevilacqua, M. Czakon, C. G. Papadopoulos, and M. Worek, Phys. Rev. Lett. **104**, 162002 (2010).
[9] G. Bevilacqua, M. Czakon, C. G. Papadopoulos, and M. Worek, Phys. Rev. D **84**, 114017 (2011).
[10] S. Hoeche, F. Krauss, P. Maierhoefer, S. Pozzorini, M. Schonherr, and F. Siegert, Phys. Lett. B **748**, 74 (2015).
[11] S. Höche, P. Maierhöfer, N. Moretti, S. Pozzorini, and F. Siegert, Eur. Phys. J. C **77**, 145 (2017).
[12] C. Gütschow, J. M. Lindert, and M. Schönherr, Eur. Phys. J. C **78**, 317 (2018).

[13] A. Bredenstein, A. Denner, S. Dittmaier, and S. Pozzorini, Phys. Rev. Lett. **103**, 012002 (2009).
[14] G. Bevilacqua, M. Czakon, C. G. Papadopoulos, R. Pittau, and M. Worek, J. High Energy Phys. 09 (2009) 109.
[15] A. Bredenstein, A. Denner, S. Dittmaier, and S. Pozzorini, J. High Energy Phys. 03 (**2010**) 021.
[16] F. Buccioni, S. Kallweit, S. Pozzorini, and M. F. Zoller, J. High Energy Phys. 12 (**2019**) 015.
[17] G. Bevilacqua, H.-Y. Bi, H. B. Hartanto, M. Kraus, M. Lupattelli, and M. Worek, Phys. Rev. D **107**, 014028 (2023).
[18] A. Denner, J.-N. Lang, and M. Pellen, Phys. Rev. D **104**, 056018 (2021).
[19] G. Bevilacqua, H.-Y. Bi, H. B. Hartanto, M. Kraus, M. Lupattelli, and M. Worek, J. High Energy Phys. 08 (2021) 008.
[20] K. Melnikov, A. Scharf, and M. Schulze, Phys. Rev. D **85**, 054002 (2012).
[21] G. Bevilacqua, H. B. Hartanto, M. Kraus, and M. Worek, Phys. Rev. Lett. **116**, 052003 (2016).
[22] G. Bevilacqua, H. B. Hartanto, M. Kraus, and M. Worek, J. High Energy Phys. 11 (**2016**) 098.
[23] G. Bevilacqua, H. B. Hartanto, M. Kraus, M. Schulze, and M. Worek, J. High Energy Phys. 03 (2018) 169.
[24] A. Kardos, C. Papadopoulos, and Z. Trocsanyi, Phys. Lett. B **705**, 76 (2011).
[25] S. Alioli, S.-O. Moch, and P. Uwer, J. High Energy Phys. 01 (2012) 137.
[26] A. Kardos and Z. Trócsányi, J. Phys. G **41**, 075005 (2014).
[27] F. Cascioli, P. Maierhöfer, N. Moretti, S. Pozzorini, and F. Siegert, Phys. Lett. B **734**, 210 (2014).
[28] M. V. Garzelli, A. Kardos, and Z. Trócsányi, J. High Energy Phys. 03 (2015) 083.
[29] M. Czakon, H. B. Hartanto, M. Kraus, and M. Worek, J. High Energy Phys. 06 (**2015**) 033.
[30] G. Bevilacqua, M. V. Garzelli, and A. Kardos, arXiv: 1709.06915.
[31] T. Ježo, J. M. Lindert, N. Moretti, and S. Pozzorini, Eur. Phys. J. C **78**, 502 (2018).
[32] CMS Collaboration, Report No. CMS-PAS-TOP-20-006, 2022, https://cds.cern.ch/record/2803771.
[33] K. Melnikov and M. Schulze, J. High Energy Phys. 08 (2009) 049.
[34] J. M. Campbell and R. K. Ellis, J. Phys. G **42**, 015005 (2015).
[35] A. Behring, M. Czakon, A. Mitov, A. S. Papanastasiou, and R. Poncelet, Phys. Rev. Lett. **123**, 082001 (2019).
[36] M. Czakon, A. Mitov, and R. Poncelet, J. High Energy Phys. 05 (2021) 212.
[37] G. Bevilacqua, M. Czakon, M. V. Garzelli, A. van Hameren, A. Kardos, C. G. Papadopoulos, R. Pittau, and M. Worek, Comput. Phys. Commun. **184**, 986 (2013).
[38] G. Ossola, C. G. Papadopoulos, and R. Pittau, Nucl. Phys. **B763**, 147 (2007).
[39] G. Ossola, C. G. Papadopoulos, and R. Pittau, J. High Energy Phys. 03 (2008) 042.
[40] A. van Hameren, C. G. Papadopoulos, and R. Pittau, J. High Energy Phys. 09 (2009) 106.
[41] P. Draggiotis, M. V. Garzelli, C. G. Papadopoulos, and R. Pittau, J. High Energy Phys. 04 (2009) 072.
[42] A. van Hameren, Comput. Phys. Commun. **182**, 2427 (2011).
[43] G. Bevilacqua, H. B. Hartanto, M. Kraus, T. Weber, and M. Worek, J. High Energy Phys. 03 (2020) 154.
[44] S. Actis, A. Denner, L. Hofer, A. Scharf, and S. Uccirati, J. High Energy Phys. 04 (**2013**) 037.
[45] S. Actis, A. Denner, L. Hofer, J.-N. Lang, A. Scharf, and S. Uccirati, Comput. Phys. Commun. **214**, 140 (2017).
[46] A. Denner, S. Dittmaier, and L. Hofer, Comput. Phys. Commun. **212**, 220 (2017).
[47] A. Denner, S. Dittmaier, M. Roth, and D. Wackeroth, Nucl. Phys. **B587**, 67 (2000).
[48] E. Accomando, A. Denner, and A. Kaiser, Nucl. Phys. **B706**, 325 (2005).
[49] A. Denner and M. Pellen, J. High Energy Phys. 08 (2016) 155.
[50] P. Draggiotis, R. H. P. Kleiss, and C. G. Papadopoulos, Phys. Lett. B **439**, 157 (1998).
[51] P. D. Draggiotis, R. H. P. Kleiss, and C. G. Papadopoulos, Eur. Phys. J. C **24**, 447 (2002).
[52] G. Bevilacqua, M. Czakon, M. Kubocz, and M. Worek, J. High Energy Phys. 10 (**2013**) 204.
[53] S. Catani and M. H. Seymour, Nucl. Phys. **B485**, 291 (1997); **B510**, 503(E) (1998).
[54] S. Catani, S. Dittmaier, M. H. Seymour, and Z. Trocsanyi, Nucl. Phys. **B627**, 189 (2002).
[55] M. Czakon, C. G. Papadopoulos, and M. Worek, J. High Energy Phys. 08 (2009) 085.
[56] L. Basso, S. Dittmaier, A. Huss, and L. Oggero, Eur. Phys. J. C **76**, 56 (2016).
[57] M. Jezabek and J. H. Kuhn, Nucl. Phys. **B314**, 1 (1989).
[58] A. Denner, S. Dittmaier, S. Kallweit, and S. Pozzorini, J. High Energy Phys. 10 (**2012**) 110.
[59] A. Buckley, J. Ferrando, S. Lloyd, K. Nordström, B. Page, M. Rüfenacht, M. Schönherr, and G. Watt, Eur. Phys. J. C **75**, 132 (2015).
[60] R. D. Ball *et al.* (NNPDF Collaboration), Eur. Phys. J. C **77**, 663 (2017).
[61] S. Bailey, T. Cridge, L. A. Harland-Lang, A. D. Martin, and R. S. Thorne, Eur. Phys. J. C **81**, 341 (2021).
[62] T.-J. Hou *et al.*, Phys. Rev. D **103**, 014013 (2021).
[63] R. D. Ball *et al.* (PDF4LHC Working Group), J. Phys. G **49**, 080501 (2022).
[64] M. Cacciari, G. P. Salam, and G. Soyez, J. High Energy Phys. 04 (2008) 063.